A New Approach Methodology (NAM) for the Prediction of (Nor)Ibogaine-Induced Cardiotoxicity in Humans

Miaoying Shi, Sebastiaan Wesseling, Hans Bouwmeester and Ivonne M. C. M. Rietjens
Division of Toxicology, Wageningen University and Research, Wageningen, The Netherlands

Abstract

The development of non-animal-based new approach methodologies (NAMs) for chemical risk assessment and safety evaluation is urgently needed. The aim of the present study was to investigate the applicability of an *in vitro-in silico* approach to predict human cardiotoxicity of the herbal alkaloid ibogaine and its metabolite noribogaine, which are promising anti-addiction drugs. Physiologically based kinetic (PBK) models were developed using *in silico*-derived parameters and biokinetic data obtained from *in vitro* liver microsomal incubations and Caco-2 transport studies. Human induced pluripotent stem cell-derived cardiomyocytes combined with a multi-electrode array (MEA) assay were used to determine *in vitro* concentration-dependent cardiotoxicity reflected by prolongation of field potential duration, which was subsequently translated to *in vivo* dose-dependent prolongation of the QTc (heart rate corrected duration from ventricular depolarization to repolarization) using PBK modeling-based reverse dosimetry. Results showed that the predictions matched well with *in vivo* kinetic data and QTc data for ibogaine and noribogaine available in the literature, indicating a good performance of the NAM. Benchmark dose analysis of the predicted dose response curves adequately predicted the onset of *in vivo* cardiotoxicity detected by QTc prolongation upon oral exposure to ibogaine and noribogaine. The present study provides an additional proof-of-principle of using PBK modeling-based reverse dosimetry as a NAM to predict human cardiotoxicity.

1 Introduction

In line with the 3Rs principle, the development of non-animal-based novel methods towards new approach methodologies (NAMs) for chemical risk assessment and safety evaluation has become a leading research topic (Andersen et al., 2019; ICCVAM, 2018; Taboureau et al., 2020). NAMs based on *in vitro* and *in silico* models generate data with high throughput and reduce animal use and costs in predicting human toxicity (Bos et al., 2020; Patterson et al., 2020). Within the framework of NAMs, *in vitro* toxicity assays characterize the biological effects of chemicals with a target organ specificity that reflects the relevant mode of action, while *in vitro* and/or computational models can capture the biokinetics related to absorption, distribution, metabolism, and excretion (ADME) (Andersen et al., 2019; Punt et al., 2020). One good example of such a NAM approach is so-called physiologically based kinetic (PBK) modeling-based reverse dosimetry, which has been shown to be of use for quantitative *in vitro* to *in vivo* extrapolation (QIVIVE), enabling the

definition of *in vivo* dose response curves for different toxic endpoints (Abdullah et al., 2016; Gilbert-Sandoval et al., 2020; Louisse et al., 2010; Rietjens et al., 2011; Strikwold et al., 2017; Zhao et al., 2019) including cardiotoxicity (Shi et al., 2020a).

In our previous work, we demonstrated that *in vivo* methadone-induced QTc prolongation (heart rate corrected duration from ventricular depolarization to repolarization) can be adequately predicted based on *in vitro* cardiotoxic effects of methadone on human induced pluripotent stem cell-derived cardiomyocytes (hiPSC-CMs) combined with PBK modeling (Shi et al., 2020a). Given that cardiotoxicity is one of the most common toxic endpoints and a main reason for discontinuing drug development (Ovics et al., 2020; Pang et al., 2019), it is of importance to validate the applicability and accuracy of this newly developed NAM by providing additional proof of principle for its prediction of cardiotoxicity. Thus, the aim of the present study was to apply the developed PBK modeling-based reverse dosimetry approach to predict the potential cardiotoxicity of ibogaine and its metabolites, which are plant-based substances that have attracted spe-

Correspondence: Ivonne Rietjens
Division of Toxicology, Wageningen University
Stippeneng 4, 6708 WE Wageningen, The Netherlands
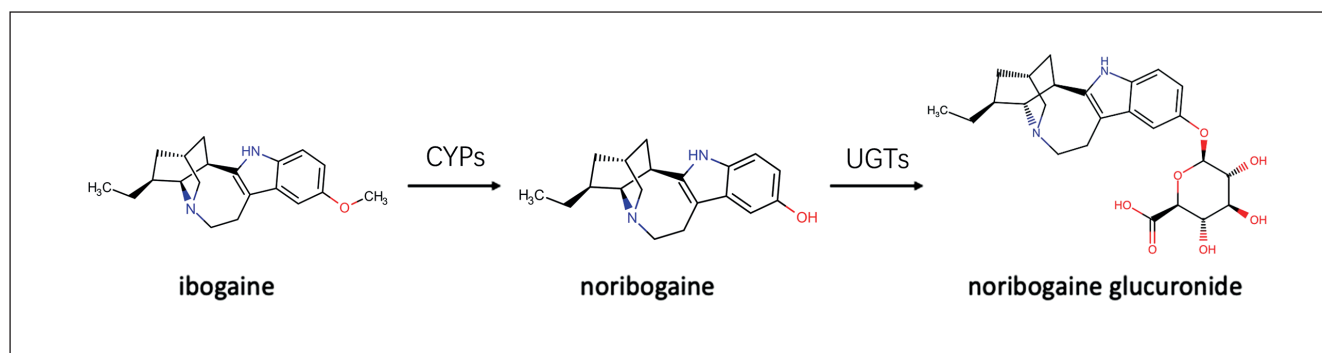(ivonne.rietjens@wur.nl)

Fig: 1: Metabolization of ibogaine to noribogaine by P450 cytochromes (CYPs) and subsequent conversion of noribogaine to noribogaine glucuronide by glucuronosyltransferases (UGTs)

cial attention due to cardiotoxicity occurring in the clinical setting (Schep et al., 2016).

Ibogaine is an indole alkaloid naturally occurring in the West African shrub *Tabernanthe iboga*, which was used as a traditional medicine and at religious ceremonies (Davis et al., 2017; Goutarel et al., 1993; Litjens and Brunt, 2016; Mash et al., 2018). Nowadays, ibogaine is banned or allowed only under medical supervision in most countries except for New Zealand due to its psychoactive properties (Noller et al., 2018). A single high dose of ibogaine can reduce drug-induced withdrawal symptoms in humans (Alper et al., 1999; Mash et al., 2018; Noller et al., 2018). Ibogaine is mainly metabolized by hepatic P450 cytochromes (CYPs) via O-demethylation to the primary metabolite noribogaine, which is also psychoactive and has pharmacological effects (Obach et al., 1998; Glue et al., 2016; Mash et al., 2016; Litjens and Brunt, 2016). The major enzyme involved in the conversion of ibogaine to noribogaine has been identified in both *in vitro* and *in vivo* studies to be CYP2D6 (Obach et al., 1998; Glue et al., 2015b), with minor contributions from CYP2C9 and CYP3A4 (Obach et al., 1998). Subsequently, noribogaine is cleared via glucuronidation to noribogaine glucuronide (Glue et al., 2015a,b, 2016) (Fig. 1).

The efficacy and safety of ibogaine and noribogaine for the treatment of drug addiction has been under debate for decades. Despite evidence obtained in preclinical and clinical studies showing promising pharmacological efficacy, cardiotoxicity was identified as the major safety concern for its clinical use (Schep et al., 2016). Several fatalities and case reports describe patients who received a high dose of ibogaine after which they experienced prolonged QTc intervals that could further develop to cardiac arrythmia and even sudden death (Asua, 2013; Grogan et al., 2019; Hildyard et al., 2016; Hoelen et al., 2009; O'Connell et al., 2015; Paling et al., 2012; Pleskovic et al., 2012; Steinberg and Deyell, 2018; Vlaanderen et al., 2014). Furthermore, Glue et al. (2016) observed a dose-dependent effect of

noribogaine on QTc prolongation in opioid-dependent patients. The observed QT prolongation could be associated with the potential inhibitory effect of both compounds on human ether-à-go-go-related gene (hERG) channels that play a critical role in cardiac repolarization (Martin et al., 2004). Based on *in vitro* studies using the electrophysiological-based patch clamp technique, both ibogaine and noribogaine were reported to block the hERG channels with similar potency (Alper et al., 2016; Koenig et al., 2014; Rubi et al., 2017).

In the present study, to predict cardiotoxicity upon oral exposure to ibogaine or noribogaine using PBK modeling-based reverse dosimetry, the *in vitro* cardiotoxicity of the two compounds was quantified in hiPSC-CMs using the multiple-electrode array (MEA) technique. This data was combined with *in vitro* biokinetic data and used in a PBK modeling-based reverse dosimetry approach to predict human dose-response curves. The hiPSC-CM MEA assay quantifies the extracellular field potential duration corrected for beat rate (FPDc) as an *in vitro* surrogate of QTc prolongation in the human electrocardiogram (ECG). The biokinetic data describing absorption and metabolism of ibogaine and noribogaine obtained from *in vitro* experiments were integrated in a PBK model for ibogaine with a submodel for noribogaine in humans. Subsequently, the PBK model was used to translate the *in vitro* concentration-dependent cardiotoxicity to the predicted dose-dependent cardiotoxic effects on QTc prolongation. The obtained data were compared to reported human *in vivo* data on ibogaine and noribogaine-induced QTc prolongation. Benchmark dose (BMD) analysis of the predicted *in vivo* dose-response curves was performed to allow comparison to available data on human cardiotoxicity and validate the predictions. From the predicted dose-response curve, points of departure (PoDs) can be derived to define a safe level of exposure and to evaluate the risk by comparing the PoD values with exposure levels, thus providing insight into the use of the NAM to evaluate the risk of ibogaine and noribogaine-induced cardiotoxicity in the clinical setting.

Abbreviations

ADME, absorption, distribution, metabolism and excretion; BMC, benchmark concentration; BMCL$_{10}$, lower 95% confidence limit of the benchmark concentration resulting in 10% effect above background; BMD, benchmark dose; BMDL$_{10}$, lower 95% confidence limit of the BMD resulting in 10% effect above background; CYP, cytochrome P450; ECG, electrocardiogram; FPDc, field potential duration corrected for beat rate; hERG, human ether-à-go-go-related gene; hiPSC-CM, human induced pluripotent stem cell-derived cardiomyocytes; MEA, multi-electrode array; NAM, new approach methodology; QIVIVE, quantitative *in vitro* to *in vivo* extrapolation
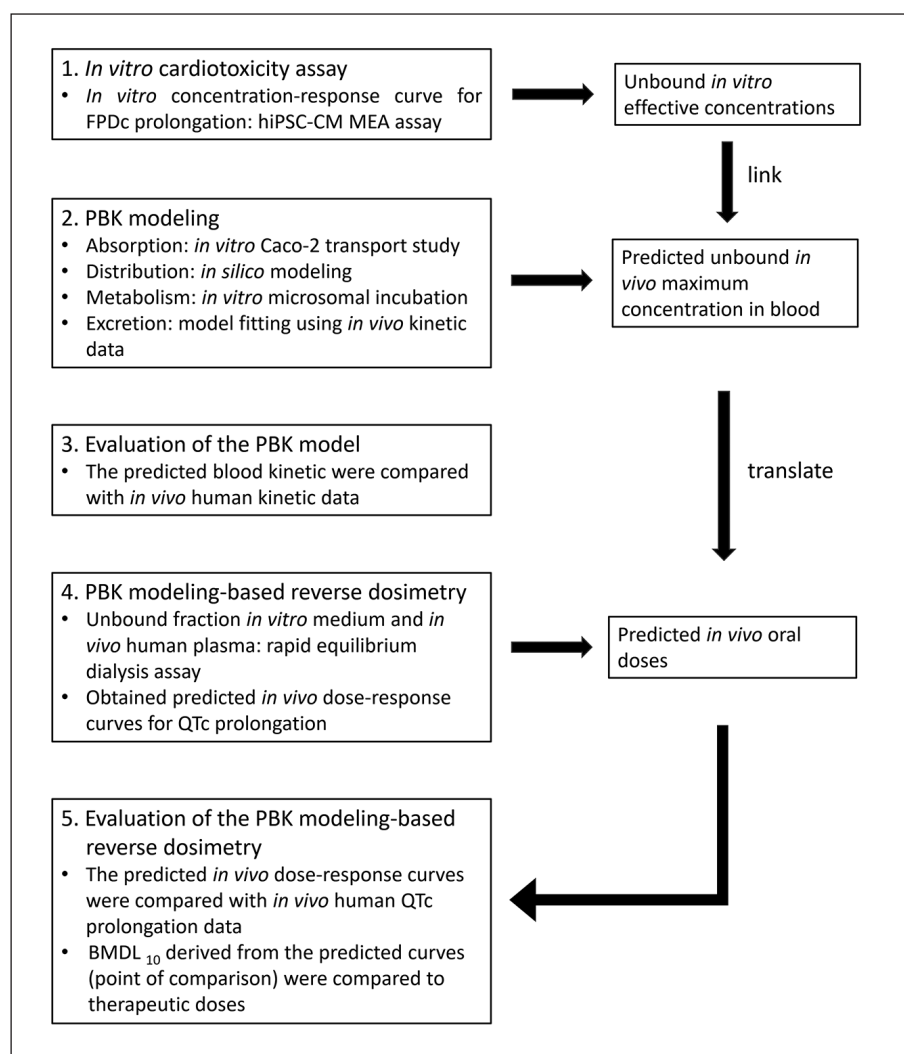
Fig. 2: General outline of the PBK modeling-based reverse dosimetry approach

BMCL$_{10}$, lower 95% confidence limit of the benchmark concentration resulting in 10% effect above background; FPDc, field potential duration corrected for beat rate; hiPSC-CM, human induced pluripotent stem cell-derived cardiomyocytes; MEA, multi-electrode array; PBK, physiologically based kinetic; QTc, (heart rate corrected duration from ventricular depolarization to repolarization).

2 Materials and methods

2.1 Chemicals and biological materials

Ibogaine hydrochloride (99.5%), noribogaine hydrochloride (98.8%) and noribogaine glucuronide lithium salt (97.4%) were purchased from TLC Pharmaceutical Standards Ltd. (Newmarket, Ontario, Canada). Antipyrine ($\geq$ 99%), bovine serum albumin (BSA, $\geq$ 96%), dofetilide ($\geq$ 98%), fibronectin, fluorescein (95%), isoproterenol hydrochloride ($\geq$ 98%), methadone hydrochloride ($\geq$ 98%), methanesulfonic acid ($\geq$ 99%) and tris(hydroxymethyl)aminomethane (Tris) were purchased from Sigma-Aldrich (Zwijndrecht, The Netherlands). Methadone was used under the opium exemption license number 104783 03 WCO registered at Farmatec (executive organization of the Ministry of Health, Welfare and Sport, The Hague, The Netherlands). Dimethyl sulfoxide (DMSO, 99.7%) and sodium hydrogen carbonate (NaHCO$_3$, $\geq$ 99%) were obtained from Merck (Schiphol-Rijk, The Netherlands). Acetonitrile (UPLC/MS grade) was obtained from Biosolve BV (Valkenswaard, The Netherlands). For-

mic acid (FA) was purchased from VWR International (Amsterdam, The Netherlands).

hiPSC-CM (Pluricyte® cardiomyocytes, cat# PCMI-1031-1) and Pluricyte® Cardiomyocyte Medium were purchased from Ncardia (Leiden, The Netherlands). The human colon carcinoma cell line Caco-2 was obtained from ATCC (Manassas, VA, USA). Dulbecco's modified Eagle's medium (DMEM, GlutaMAX™ containing 4.5 g/L D-glucose and pyruvate), Hank's balanced salt solution (HBSS) without phenol red and phosphate-buffered saline (PBS) were obtained from Gibco (Paisley, Scotland, UK). Non-essential amino acids (NEAA) and penicillin-streptomycin (P/S) were purchased from Gibco (Grand Island, New York, USA). Fetal bovine serum (FBS) was purchased from Bodinco BV (Alkmaar, The Netherlands). Pooled human liver microsomes (Corning® UltraPool™ HLM 150, pooled from 150 donors with mixed gender), reduced nicotinamide adenine dinucleotide phosphate (NADPH) regenerating system solution A and solution B, and glucuronosyltransferase (UGT) reaction mix system solution A and solution B were purchased from Corning
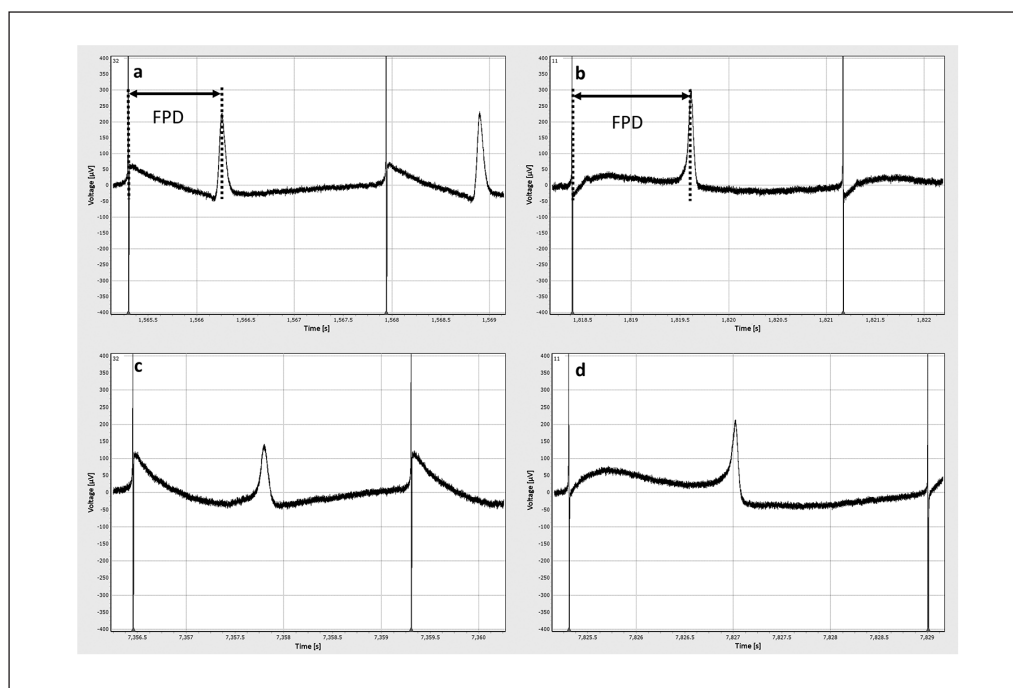
Fig. 3: Normal and prolonged waveforms of field potential observed in human induced pluripotent stem cell-derived cardiomyocytes using a multiple-electrode array
(a) Field potential duration (FPD) at baseline condition with the treatment of 0.05% (v/v) acetonitrile. (b) FPD at baseline condition with the treatment of 0.1% (v/v) DMSO. (c) Prolonged FPD observed at 0.4 μM ibogaine. (d) Prolonged FPD observed at 0.4 μM noribogaine.

(Woburn, MA, USA). Pooled human plasma and rapid equilibrium dialysis (RED) materials, including RED inserts, RED base plates and sealing tape, were obtained from Thermo Fisher Scientific (Bleiswijk, The Netherlands).

2.2 General outline of the PBK modeling-based reverse dosimetry approach

The PBK modeling-based reverse dosimetry approach to predict *in vivo* dose-response curves from *in vitro* cardiotoxicity concentration-response data included the following steps: i) establishment of the *in vitro* concentration-response curves for ibogaine and its metabolite noribogaine in hiPSC-CM using the MEA, ii) development of a PBK model for ibogaine and noribogaine in humans using biokinetic data obtained from *in vitro* liver microsomal incubations and Caco-2 transport studies, and parameters derived from *in silico* simulations and the literature, iii) evaluation of the PBK model, iv) translation of *in vitro* concentration-response curves to *in vivo* dose-response curves using the PBK model, and v) evaluation of the PBK modeling-based reverse dosimetry approach by comparing predicted dose-response data to data obtained from the literature on the effects of ibogaine and noribogaine on QTc prolongation. The general outline of the PBK modeling-based reverse dosimetry approach is illustrated in Figure 2.

2.3 *In vitro* cardiotoxicity of ibogaine and noribogaine in the hiPSC-CM MEA assay

Exposure and MEA recording
The exposure and recording of the spontaneous beating of hiPSC-CMs was conducted as previously described (Shi et al.,

2020a). Stock solutions of ibogaine were prepared in acetonitrile/water (50/50 v/v). Noribogaine and two reference substances, dofetilide and isoproterenol, were dissolved in DMSO. All stock solutions were diluted in culture medium to make exposure medium with a final concentration of 0.05% (v/v) acetonitrile or 0.1% (v/v) DMSO. Based on cytotoxicity and relevant human plasma concentrations observed upon oral administration of ibogaine and noribogaine, the following concentrations were tested: 0 (control), 0.03, 0.1, 0.2, 0.3, 0.4, 0.5, 1 μM (ibogaine) and 0 (control), 0.03, 0.1, 0.2, 0.3, 0.4, 1, 3 μM (noribogaine). The test concentrations were 0 (control), 0.1, 0.3, 1, 3, 10 nM for dofetilide and 0 (control), 3, 10, 30, 100, 300 nM for isoproterenol, which are typical responsive concentrations in the hiPSC-CM MEA assay (Zwartsen et al., 2019).

The precoating of MEA chips (60-6well MEA200/30iR-Ti-tcr, MCS GmbH, Reutlingen, Germany) and the culturing of Pluricyte® cardiomyocytes were done according to the manufacturer's protocol as previously described in Shi et al. (2020a). At day 7-9 post-seeding, extracellular field potentials of cardiomyocytes (Fig. 3) were accessed using the MEA2100-system (MCS GmbH) equipped with a chamber and a heating controller that guaranteed a stable atmosphere (37°C with 5% CO_2). Cells were equilibrated for 20 min prior to the compound/vehicle exposure. Measurements started by replacing half of the medium in each well with fresh medium containing 0.1% (v/v) acetonitrile or 0.2% (v/v) DMSO to reach a final concentration of 0.05% (v/v) acetonitrile or 0.1% (v/v) DMSO, which was defined as baseline condition. Following the same procedure, each concentration of the model compounds was cumulatively added to the well, increasing the concentration at each subsequent addition (Ando et al., 2017; Nozaki et al., 2017). In each MEA chip, five of the six wells were

exposed to model or reference compounds while one well served as the vehicle control analyzed during a similar period as the other wells to enable corrections for time-, addition- and vehicle-dependent effects on the field potentials. At each concentration, exposure was conducted for 15 min followed by a 2 min recording of extracellular field potentials. Data were recorded using Cardio 2D 2.12.0 software (MCS GmbH) with a sample frequency of 10 kHz and a 0.1-3.5 kHz band-pass filter.

Data analysis and statistics
Raw data obtained from the hiPSC-CM MEA assay was analyzed using MultiwellAnalyzer 1.8.6.0 software (MCS GmbH). Electrodes with field potentials of good quality, i.e., those with amplitudes of depolarization and repolarization peaks higher than 200 µV and 20 µV, respectively, were selected for further analysis (Ando et al., 2017; Sala et al., 2017; Shi et al., 2020a). Subsequently, two parameters reflecting electrophysiological activity of cardiomyocytes, namely field potential duration (FPD, duration between the beginning of the sodium spike and the repolarizing peak) and RR interval (duration between two depolarization peaks), were measured from the 2 min recording for each concentration.

In line with other MEA studies, the Fridericia formula (Eq. 1) was applied to correct for the effect of beat rate on FPD (Ando et al., 2017; Kitaguchi et al., 2017; Vandenberk et al., 2016):

$$FPDc = \frac{FPD}{\sqrt[3]{RR \text{ interval}}} \qquad \text{Eq. 1}$$

where the FPD and RR-interval are expressed in seconds.

Well-based FPDc were determined by calculating the relative percentage of FPDc for the exposure measurements compared to FPDc at baseline conditions (0.05% (v/v) acetonitrile or 0.1% (v/v) DMSO) set at 100%. The potential effects of time, addition, and vehicle on well-based FPDc were corrected for by subtracting the responses obtained from the corresponding time-matched vehicle control well. Irregular waveforms (Fig. S1[1]) of the field potential including arrhythmia-type changes, a flattened unclear second peak, and beating arrest may occur at high concentrations (Kitaguchi et al., 2017; Shi et al., 2020a; Zwartsen et al., 2019). For deriving concentration-response curves of model compounds, concentrations inducing irregular waveforms were excluded as the FPD and RR interval could not be defined.

To compare the potency of model compounds, BMD analysis was used to derive effective concentrations causing a defined % increase in the FPDc compared to the baseline control as described in the "Benchmark dose analysis" section. The concentration-response curves were plotted using GraphPad Prism 5.0 with four-parameter logistic fit (GraphPad Software Inc., San Diego, USA). Data were collected from three independent experiments with six well replicates (two replicates for dofetilide and isoproterenol) in each experiment. Each data point is presented as the mean value ± standard deviation (SD) of the three

independent replicates. One-way analysis of variance (ANOVA) followed by Dunnett's test was conducted to assess the effect of ibogaine and noribogaine on FPDc using GraphPad Prism 5.0. Significance was determined at $p < 0.05$.

2.4 *In vitro* experimental biokinetic parameters for the PBK models

In vitro *intestinal transport studies*
To estimate the intestinal absorption of ibogaine and noribogaine, a Caco-2 transport study was performed to determine the apparent permeability coefficients (P_{app}) using a previously developed method with minor modifications (Hubatsch et al., 2007; Strikwold et al., 2017). Caco-2 cells (passages 10-15 post-thawing) were seeded onto the inserts of Costar 12-well transwell plates (Corning, 0.4 µm pored polycarbonate membrane, 12 mm diameter). The apical compartment of each well was filled with 0.5 mL of a 4 x 10^4 cell suspension in culture medium consisting of DMEM supplemented with 10% (v/v) FBS, 1% (v/v) P/S and 1% (v/v) NEAA, and the basolateral compartment was filled with 1.5 mL culture medium. Given that FBS is an animal-derived component, whose production may be associated with pain and suffering, FBS-free culture medium for Caco-2 cells, e.g., serum-free DMEM containing insulin, transferrin, selenium (ITS) or MITO+™ serum extender (ITS plus growth factors) (Ferruzza et al., 2013), could be considered for future Caco-2 transport studies. The plate was incubated under atmospheric conditions at 37°C and 5% CO$_2$ for 21-23 days, which allows cells to grow and differentiate into a confluent monolayer. Cell culture medium was changed every 2 days.

Stock solutions of ibogaine were prepared in acetonitrile/water (50/50 v/v). Noribogaine, methadone (reference compound), antipyrine (passive transcellular control for the transport studies) and fluorescein (passive paracellular control for the transport studies) were dissolved in DMSO. Stock solutions were diluted 200-fold resulting in a final test concentration of 50 µM (125 nM for fluorescein) at which cytotoxicity was not observed (data not shown). The final concentration of acetonitrile or DMSO was 0.25% (v/v) or 0.5% (v/v), respectively.

For the transport experiment, HBSS containing 10 mM methanesulfonic acid, NaHCO$_3$ (final concentration 0.35 mg/mL) and the respective test compounds was used as exposure medium (pH 6.5) in the apical compartment. HBSS containing 30 mg/mL BSA was used as medium in the basolateral compartment (pH 7.4). 1.5 mL basolateral transport medium was added first, and the experiment was initiated by adding 0.5 mL exposure medium to the apical compartment. The plate was incubated at 37°C with 5% CO$_2$ for 20 min. Subsequently, an aliquot of 75 µL sample was collected from the basolateral compartment and transferred to a tube containing 150 µL ice-cold acetonitrile. To measure the mass balance (recovery), 75 µL exposure buffer was also collected from the apical compartment before and after the incubation and added to the tubes containing 150 µL ice-cold acetonitrile. The insert fil-

ters were washed with PBS, then cut out and transferred to 200 μL ice-cold acetonitrile for a 15 min sonication. Samples were left on ice for 20 min and centrifuged for 45 min at 18,000 x g, after which supernatants were collected for LC-MS/MS analysis.

To check the linearity of transport of test compounds, 75 μL sample was collected from the basolateral compartment at 1, 5, 10, 20, 30 and 60 min of incubation and added to 150 μL ice-cold acetonitrile. After each collection, an equal volume of basolateral transport medium was added back as compensation. The calculation for each time point was corrected for the dilutions.

The integrity of the Caco-2 cell monolayer was checked by measuring the transepithelial electrical resistance (TEER) using a Millicell ERS-2 Volt-Ohm meter (EMD Millipore Corporation, California, USA). Prior to the transport experiment, cells with a TEER value between 600 and 800 Ωcm^2 were selected for the transport study. After the experiment, cells with a change in the TEER value of more than 20% were excluded from further analysis of the P_{app} value (Bentz et al., 2013). Additionally, the integrity was checked by measuring the transport of fluorescein, and cells with a transport of fluorescein lower than 1% were considered suitable for the analysis.

The P_{app} (cm/s) value was calculated using Eq. 2 as follows (Hubatsch et al., 2007; Strikwold et al., 2017):

$$P_{app} = \frac{\Delta Q / \Delta t}{A \times C_0} \qquad \text{Eq. 2}$$

where $\Delta Q/\Delta t$ (nmol/s) is the amount of the test compound transported to the basolateral compartment over the incubation time, A (cm²) is the surface area of the filter, and C_0 (μM) is the initial concentration of the test compound in the apical compartment.

The mass balance was calculated by comparing the total amount of compound in the apical compartment, basolateral compartment, and filter to the initial amount. The results were obtained from three independent experiments including four replicates for ibogaine and noribogaine and two replicates for methadone and antipyrine in each independent experiment. Data are presented as the mean value ± SD.

Using methadone as a reference compound, the *in vivo* oral absorption rate constant (ka) for ibogaine and noribogaine were calculated by multiplying the corresponding ratio of P_{app} to P_{app} of methadone by 0.59/h, which is the mean ka value of methadone reported in human studies (Foster et al., 2000; Wolff et al., 2000).

In vitro *microsomal incubations*
To determine kinetic parameters for the conversion of ibogaine to noribogaine, *in vitro* microsomal incubations were performed as described before (Shi et al., 2020a) with minor modifications. Incubation mixtures contained the NADPH regeneration system (final concentrations: 1.3 mM NADP+, 3.3 mM glucose-6-phosphate, 0.4 U/mL glucose-6-phosphate dehydrogenase and 3.3 mM MgCl₂) and ibogaine at final concentrations from 0 to 25 μM in 100 mM Tris-HCl buffer (pH 7.4) with a total volume of 160 μL. Stock solutions of ibogaine were prepared in acetonitrile/water (50/50 v/v) and were diluted 50-fold to result in the designated test concentrations in the incubation mixtures. Samples were pre-in-

cubated at 37°C for 1 min, and a final concentration of 0.25 mg/mL liver microsomal protein was added to initiate the reaction. After 2.5 min incubation in a shaking water bath at 37°C, the reaction was terminated by adding 40 μL ice-cold acetonitrile. Control incubations were performed in the absence of NADPH, which was replaced with Tris-HCl.

The formation of the glucuronide of noribogaine was investigated in a similar manner as described above. A total volume of 200 μL sample contained (final concentrations) UGT reaction system (5 mM uridine 5′-diphosphoglucuronic acid (UDPGA), 8 mM MgCl₂, 25 μg/mL alamethicin) and 0.5 mg/mL liver microsomal protein in 100 mM Tris-HCl (pH 7.4). Samples were placed on ice for 30 min, which allows the pore-forming peptide alamethicin to boost the glucuronidation activity (Fisher et al., 2000; Ning et al., 2017). After pre-incubating samples at 37°C for 5 min, reactions were started by adding noribogaine from 100-times concentrated stock solution in DMSO at final concentrations ranging from 0-750 μM. The incubation time was 40 min, and reactions were terminated by adding 50 μL ice-cold acetonitrile. Control incubations were performed in the absence of UDP-GA, which was replaced with Tris-HCl.

Test concentrations of ibogaine and noribogaine were chosen at relevant human plasma concentrations and enabled the determination of Michaelis-Menten kinetic parameters. Optimizations of experiments demonstrated that the reaction rates for the formation of noribogaine were linear with time up to 20 min and with protein concentration of up to 1 mg/mL. For the formation of noribogaine glucuronides, reaction rates were shown to be linear with time up to 120 min and with protein concentration up to 0.75 mg/mL. After termination, samples were centrifuged at 18,000 x g for 5 min at 4°C. The supernatant was collected for the quantification of ibogaine, noribogaine and noribogaine glucuronide by liquid chromatography-mass spectrometry (LC-MS/MS) as described in the "LC-MS/MS analysis" section.

For the kinetic analysis, the data for the formation of noribogaine and noribogaine glucuronide were fitted to the Michaelis-Menten Eq. 3 using GraphPad Prism 5.0 (GraphPad Software Inc.):

$$v = \frac{V_{max} \times [S]}{K_m + [S]} \qquad \text{Eq. 3}$$

where [S] is the substrate concentration (μM) and v is the rate of metabolite formation (nmol/min/mg protein). V_{max} is the apparent maximum velocity (nmol/min/mg protein) and K_m the apparent Michaelis-Menten constant (μM). The *in vitro* catalytic efficiency expressed in μL/min/mg microsomal protein was calculated by dividing V_{max} by K_m. Data were collected from three independent experiments, and each data point is presented as the mean value ± SD.

2.5 Determination of plasma protein and *in vitro* medium binding
The rapid equilibrium dialysis (RED) assay was conducted to determine the unbound fraction (f_u) of ibogaine and noribogaine in pooled human plasma and in the *in vitro* medium used in the

hiPSC-CM MEA assay as previously described (Shi et al., 2020a). The stock solutions of ibogaine prepared in acetonitrile/water (50/50 v/v) and noribogaine dissolved in DMSO were diluted 100-fold in human plasma or *in vitro* medium to reach the final concentration of 10 μM in test sample solutions. A 300 μL aliquot of test sample solution was added to the sample chamber, and 500 μL PBS was added to the buffer chamber of the RED insert, after which dialysis was performed on an orbital shaker at 37°C at 250 rpm for 5 h. Following dialysis, an aliquot of 25 μL was collected from both the sample and buffer chamber and diluted with 25 μL PBS (to the aliquot from the sample chamber) and plasma or *in vitro* medium (to the aliquot from the buffer chamber) to eliminate potential matrix effects. Subsequently, post-treatment samples were precipitated using 300 μL cold acetonitrile/water (50/50 v/v) and left on ice for 30 min followed by centrifugation for 45 min at 18,000 x g. Supernatants were collected for LC-MS/MS analysis. The fraction unbound (f_u) was calculated with Eq. 4 (van Liempd et al., 2011; Waters et al., 2008):

$$f_u = \frac{\text{concentration in buffer chamber}}{\text{concentration in sample chamber}} \qquad \text{Eq. 4}$$

The measurements were performed in triplicate in three independent experiments. Results are presented as the mean value ± SD.

2.6 LC-MS/MS analysis
The identification and quantification of compounds in samples from the Caco-2 transport studies, microsomal incubation and RED assay were performed by LC-MS/MS analysis using a Shimadzu Nexera XR LC-40D SR UPLC system coupled with a Shimadzu LCMS-8045 mass spectrometer (Kyoto, Japan). The compounds were separated by a Phenomenex Kinetex® C18 column (2.1 x 50 mm 1.7 μm, 100 Å) connected to a precolumn and detected by a Shimadzu LCMS-8045 triple quadrupole with electrospray ionization (ESI) interface. The instrument was operated in positive mode and multiple reaction monitoring (MRM, N_2 collision gas) mode. The MRMs of m/z 311.15 (MH⁺) to 122.2 (CE: -33 kV), m/z 311.15 (MH⁺) to 174.2 (CE: -36 kV) and m/z 311.15 (MH⁺) to 124.15 (CE: -31 kV) were used to analyze ibogaine. The MRMs of m/z 297 (MH⁺) to 122.15 (CE: -33 kV), m/z 297 (MH⁺) to 160.2 (CE: -35 kV) and m/z 297 (MH⁺) to 146.25 (CE: -45 kV) were used to analyze noribogaine. The MRMs of m/z 473.15 (MH⁺) to 297.2 (CE: -33 kV), m/z 473.15 (MH⁺) to 122.15 (CE: -54 kV) and m/z 473.15 (MH⁺) to 160.1 (CE: -50 kV) were used to analyze noribogaine glucuronide. The MRMs for methadone were m/z 310.2 (MH⁺) to 265.15 (CE: -15 kV), m/z 310.2 (MH⁺) to 105.05 (CE: -29 kV) and m/z 310.2 (MH⁺) to 77.15 (CE: -50 kV). The MRMs for antipyrine were m/z 189.1 (MH⁺) to 56.1 (CE: -35 kV), m/z 189.1 (MH⁺) to 77.2 (CE: -42 kV) and m/z 189.1 (MH⁺) to 58.2 (CE: -23 kV). The MRMs were selected based on previous studies (Chang et al., 2011; Glue et al., 2016).

Mobile phase A was nanopure water containing 0.1% (v/v) formic acid and mobile phase B was acetonitrile containing 0.1% (v/v) formic acid. A gradient elution at a flow rate of 0.3 mL/min was applied for the analysis with the program set as follows: the initial concentration was 100% mobile phase A, linearly changing to 100% mobile phase B over 7 min, which was held for 1 min. Then mobile phase B dropped to 0% over 1 min followed by equilibration of the system for 4 min. Total run time was 13 min. The injection volume was 1 μL, and the temperature of the column was kept at 40°C. The retention times for ibogaine, noribogaine, noribogaine glucuronide, methadone and antipyrine were 5.6, 5.0, 4.9, 6.3 and 5.1 min, respectively, determined using commercially available reference compounds. Quantification was performed by comparing the respective peak areas of the total ion chromatogram (TIC) to the TIC peak areas of corresponding linear calibration curves of reference compounds ($R^2 >$ 0.999) using Browser analysis in the software LabSolution (Shimadzu).

2.7 PBK models development and evaluation
A PBK model consisting of multiple organ compartments was developed to describe the ADME of ibogaine and its metabolite noribogaine upon oral administration (Fig. 4). Noribogaine has also been reported to cause the prolongation effects on the QTc interval in humans (Glue et al., 2016). Therefore, an oral administration route was included in the submodel of noribogaine (Fig. 4), which enables modeling of noribogaine kinetics and prediction of its cardiotoxicity upon oral administration. A full description of the model development can be found in Text S1 and Tables S2 and S3[1]. Kinetic model calculations were performed with Berkeley Madonna (version 8.3.18, UC Berkeley, CA, USA), applying Rosenbrock's algorithms for solving stiff systems. Model equations are shown in Text S2[1].

To evaluate the model, the predicted blood concentrations and area under the blood concentration-time curve (AUC) of ibogaine and noribogaine were compared with the *in vivo* data reported in clinical studies (Glue et al., 2015a,b, 2016). The reported plasma-based kinetics of ibogaine and noribogaine were extracted using WebPlotDigitizer Version 4.4. (Rohatgi, 2020) and converted to blood-based kinetics by multiplying with the respective blood-to-plasma ratio (BPr) values. The evaluation was performed according to the specifications (body weight and oral dose) of *in vivo* studies as summarized in Table 2. A local parameter sensitivity analysis was conducted to estimate to what extent the model parameters can influence the model output. A full description of the sensitivity analysis and results can be found in Text S3 and Figure S5[1].

2.8 QIVIVE using PBK modeling-based reverse dosimetry
Given that the *in vitro* endpoint FPDc can be considered a surrogate endpoint for the QTc interval in the human ECG (Shi et al., 2020a; Zwartsen et al., 2019), *in vitro* concentration-response curves for FPDc obtained in the hiPSC-CM MEA assay were translated to *in vivo* dose-response curves for QTc using PBK modeling-based reverse dosimetry. In the case of oral administration of ibogaine, a toxic equivalence (TEQ) approach was applied to combine the cardiotoxicity of ibogaine and noribogaine. Assuming that the cardiotoxicity of ibogaine and noribogaine are additive to hiPSC-CM, the internal unbound TEQ concentration
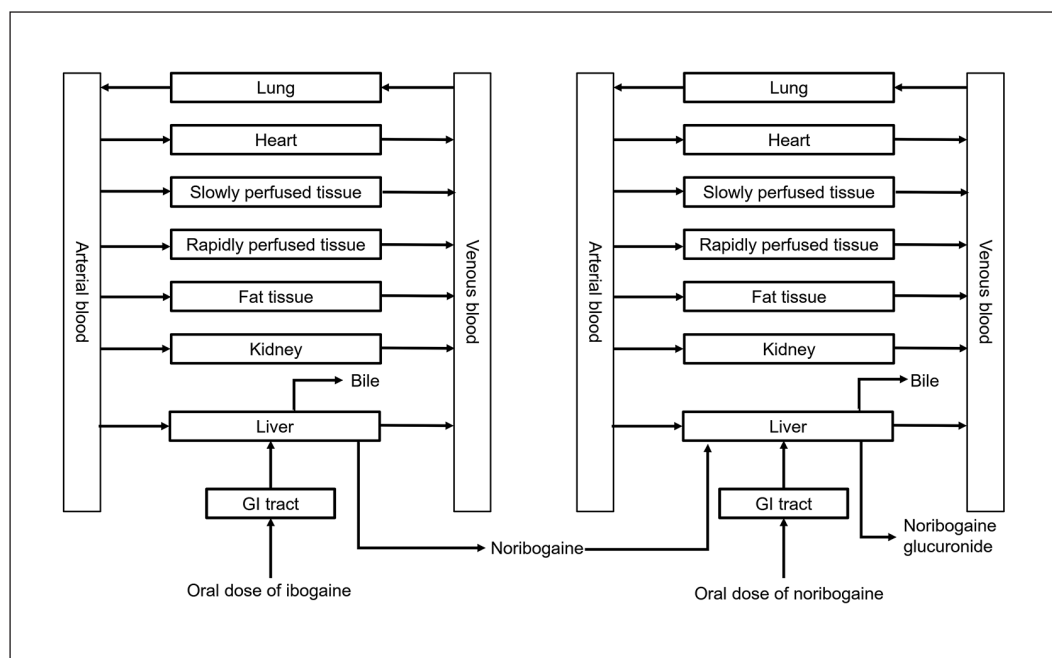
Fig. 4: Schematic diagram of the PBK model for ibogaine with a submodel for noribogaine

was the combination of the unbound concentration of ibogaine and noribogaine in the heart venous blood taking the corresponding toxic equivalency factors (TEFs) into account. The TEFs of ibogaine and noribogaine were calculated based on their cardiotoxic potencies obtained in the hiPSC-CM MEA assay, with the TEF for ibogaine defined as 1.00. Then QIVIVE was performed by assuming the *in vitro* unbound concentration of ibogaine equal to the C_{max} of unbound ibogaine expressed in TEQ concentrations in the heart venous blood as shown in Eq. 5 and 6:

$$C_{total,\textit{in vitro},ibo} \times f_{u,m,ibo} = C_{unbound,human\ blood,TEQ} \qquad \text{Eq. 5}$$

$$
\begin{aligned}
C_{unbound,human\ blood,TEQ} = \\
C_{total,human\ blood,ibo} \times \frac{f_{u,p,ibo}}{BPr_{ibo}} \times TEF_{ibo} \\
+ \ C_{total,human\ blood,nor} \times \frac{f_{u,p,nor}}{BPr_{nor}} \times TEF_{nor}
\end{aligned}
\qquad \text{Eq. 6}
$$

where $C_{total,\textit{in vitro},ibo}$ and $f_{u,m,ibo}$ are the *in vitro* ibogaine concentration and unbound fraction of ibogaine in the *in vitro* exposure medium, respectively. BPr_{ibo} and BPr_{nor} are the blood to plasma ratio of ibogaine and noribogaine. $f_{u,p,ibo}$ and $f_{u,p,nor}$ are the respective unbound fraction of ibogaine and noribogaine in human plasma. $C_{total,human\ blood,ibo}$ and $C_{total,human\ blood,nor}$ are the concentrations of ibogaine and noribogaine in the heart venous blood, respectively. TEF_{ibo} and TEF_{nor} are the TEF values of ibogaine (defined as 1.00) and noribogaine (defined based on its relative potency in the MEA assay). $C_{unbound,human\ blood,TEQ}$ values were converted to *in vivo* oral doses of ibogaine by PBK modeling-based reverse dosimetry, using a body weight of 70 kg (Brown et al., 1997).

When oral administration of noribogaine was considered, the translation was performed by setting the *in vitro* unbound concentrations of noribogaine detected in the hiPSC-CM MEA assay equal to the unbound C_{max} of noribogaine in the heart venous blood with a correction for the fraction unbound in human plasma and conversion from plasma to blood using BPr as described in Eq.7:

$$C_{total,human\ blood,nor} = \frac{C_{total,\textit{in vitro},nor} \times f_{u,m,nor}}{\dfrac{f_{u,p,nor}}{BPr_{nor}}} \qquad \text{Eq. 7}$$

where $C_{total,\textit{in vitro},nor}$ and $f_{u,m,nor}$ are the *in vitro* noribogaine concentration and unbound fraction of noribogaine in the *in vitro* exposure medium, respectively. $C_{total,human\ blood,nor}$ values were extrapolated to *in vivo* oral doses of noribogaine by PBK modeling-based reverse dosimetry, using a body weight of 70 kg (Brown et al., 1997). The calculations using Eq. 5 and 6 or 7 were performed for each of the *in vitro* concentrations of ibogaine or noribogaine tested in the hiPSC-CM MEA assay, which enables the translation of the entire *in vitro* concentration-response curve to a predicted *in vivo* dose-response curve.

2.9 Validation of the PBK modeling-based reverse dosimetry approach

To validate the performance of the PBK modeling-based reverse dosimetry approach, the predicted dose-response curves for QTc prolongation upon exposure to ibogaine and noribogaine were compared to the respective *in vivo* dose-response data obtained from case reports and clinical studies (Asua, 2013; Glue et al., 2016; Grogan et al., 2019; Henstra et al., 2017; Hildyard et al., 2016; Hoelen et al., 2009; Meisner et al., 2016; Pleskovic et

al., 2012; Steinberg and Deyell, 2018; Vlaanderen et al., 2014). Since in most case reports ibogaine administered to the patients was internet-purchased with unknown purity, the reported doses were converted to effective doses by multiplying with the lower (15%) and upper value (50%) of purity reported in Alper et al. (2012). The predicted dose-response curve of noribogaine for the validation was made using the body weight 81.9 kg, which was the average body weight of subjects as reported in Glue et al. (2016). The details of the *in vivo* studies are summarized in Table S1[1]. The *in vitro* absolute FPDc values and the *in vivo* QTc data were expressed as relative percentages by comparing the post-treatment data to the baseline values for a straightforward comparison.

2.10 Benchmark dose analysis

BMD analysis of reported and predicted dose-response curves for ibogaine and noribogaine was performed to derive a lower 95% confidence limit of the BMD resulting in 10% cardiotoxicity ($BMDL_{10}$), which can be used as the point of departure (PoD) for the risk assessment and safety evaluation of ibogaine and noribogaine. As previously described (Shi et al., 2020a), an effective level of 10% was chosen based on the fact that a $BMDL_{10}$ value is generally considered a dose level similar to a no observed adverse effect level (EFSA, 2017) and that 10% change in QTc interval over the population baseline of 407 ms, being a QTc of 450 ms, can be used as a threshold to evaluate the abnormal QTc prolongation (ICH, 2005; Mujtaba et al., 2013; Wedam et al., 2007; Florian et al., 2012). The European Food Safety Authority web-tool based on R-package PROAST version 69 (Dutch National Institute for Public Health and the Environment, RIVM, The Netherlands) was used for the BMD analysis (Shi et al., 2020a).

BMD analysis of *in vitro* concentration-response data was performed to calculate the benchmark concentrations (BMC) resulting in a 10% change in the FPDc with lower 95% confidence limit ($BMDL_{10}$). The obtained $BMDL_{10}$ values were used to compare the potency and derive the TEF of noribogaine relative to the TEF of ibogaine set at 1.00.

3 Results

3.1 *In vitro* cardiotoxicity of ibogaine and noribogaine in the hiPSC-CM MEA assay

Figure 5 shows that ibogaine and its metabolite noribogaine induced a significant concentration-dependent prolongation of FPDc. The $BMDL_{10}$ is 0.11 μM for ibogaine and 0.15 μM for noribogaine, which results in TEF values of ibogaine and noribogaine being 1.00 and 0.65, respectively. Arrhythmia-type waveforms were observed upon treatment with 1 μM ibogaine and 3 μM noribogaine. The repeated addition of vehicle controls (0.05% (v/v) acetonitrile and 0.1% (v/v) DMSO) did not significantly influence the FPDc (Fig. S2[1]). The two reference compounds dofetilide and isoproterenol both prolonged the FPDc and increased beat rates in a concentration-dependent manner, indicating an adequate performance of the hiPSC-CM MEA assay (Fig. S3[1]).
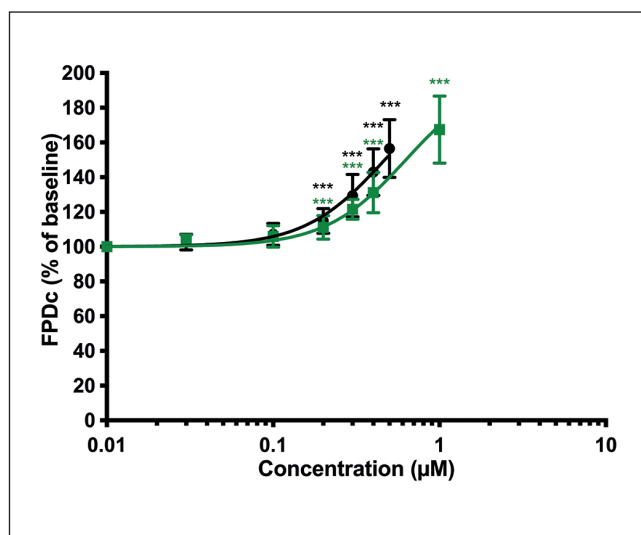

Fig. 5: Concentration-response curves of the effect of ibogaine (black circles and line) and noribogaine (green squares and line) on FPDc in hiPSC-CM detected by the MEA The response of the baseline condition (0.05% (v/v) acetonitrile for ibogaine, 0.1% (v/v) DMSO for noribogaine) was set at 100%. Data represent the mean of results obtained from three independent experiments each containing six well replicates. Each data point represents the mean ± SD. ***, p < 0.001.

3.2 *In vitro* experimental biokinetic parameters for PBK models

In vitro *intestinal transport studies*
Table 1 shows the P_{app} values obtained from Caco-2 transport studies and the ka values of the test compounds derived from these P_{app} values based on comparison to the data for methadone. All test compounds were rapidly transported with the largest P_{app} value of 47.0 x10^{-6} cm/s for antipyrine and the smallest P_{app} value of 20.8 x10^{-6} cm/s for methadone. The P_{app} value of noribogaine was 1.5-fold higher than that of ibogaine. The transport of all test compounds was within the linear range

Tab. 1: The apparent permeability (P_{app}) obtained from Caco-2 transport studies and the predicted intestinal oral absorption rate constants (ka) for the test compounds derived from the P_{app} values using the ka for methadone as the reference

Compound	P_{app} ± SD (10^{-6} cm/s)	ka (/h)
Ibogaine	27.9 ± 4.6	0.79
Noribogaine	42.4 ± 3.6	1.23
Methadone	20.8 ± 1.9	0.59[a]
Antipyrine	47.0 ± 5.0	1.33

[a] Reported value obtained from human studies (Foster et al., 2000; Wolff et al., 2000)

up to 30 min of incubation. The mass recovery of ibogaine, noribogaine, methadone and antipyrine was 90%, 102%, 74% and 88%, respectively.

In vitro *microsomal incubations*

Figure S4[1] shows the substrate concentration dependent metabolism of ibogaine and noribogaine by human liver microsomes. The obtained results follow Michaelis-Menten kinetics. The apparent V_{max} and K_m derived from these data for the formation of noribogaine from ibogaine were 0.17 ± 0.033 nmol/min/mg microsomal protein and 0.63 ± 0.005 μM, respectively. The apparent V_{max} and K_m for the conversion of noribogaine to its glucuronide were 0.036 ± 0.0008 nmol/min/mg microsomal protein and 305 ± 15.8 μM, respectively. The catalytic efficiency (V_{max}/K_m) for the formation of noribogaine was 269.8 μL/min/mg microsomal protein, which was 2,248-fold more efficient than that for formation of noribogaine glucuronide of 0.12 μL/min/mg microsomal protein. This explains the relatively higher plasma concentrations of noribogaine than of ibogaine upon dosing ibogaine (see below).

3.3 Determination of plasma protein and *in vitro* medium binding

The unbound fraction of ibogaine and noribogaine in the *in vitro* medium and human plasma were determined by the RED assay for calculation of the unbound concentration of the compounds for the *in vitro* to *in vivo* extrapolation. The unbound fractions of ibogaine and noribogaine in the *in vitro* medium were comparable, amounting to 0.71 ± 0.01 and 0.80 ± 0.03, respectively. The unbound fraction of ibogaine in human plasma was determined to be 0.04 ± 0.017, which is 6.5-fold lower than that for noribogaine (0.26 ± 0.05).

3.4 Evaluation of the PBK model

The PBK models of ibogaine and noribogaine were evaluated against *in vivo* data reported in clinical studies. Figure 6 shows that the developed PBK model accurately predicted the time-dependent change in the blood concentrations of ibogaine and noribogaine upon oral administration of ibogaine (Glue et al., 2015b) and noribogaine (Glue et al., 2015a, 2016) with differences between the predicted and reported blood C_{max} and AUC being less than around 2-fold, which is generally considered an adequate predictive performance (Badhan et al., 2019; WHO, 2010). The detailed comparisons between predicted and reported blood C_{max} and AUC values are summarized in Table 2. For ibogaine, the predicted blood C_{max} and AUC were 1.7- fold and 2.1-fold higher than the reported values, respectively. For noribogaine, the prediction shows an average 0.9-fold and 1.3-fold difference both in blood C_{max} and AUC values.

3.5 Contribution of ibogaine and noribogaine to blood ibogaine equivalents

To further illustrate the contribution of ibogaine and noribogaine to ibogaine-induced cardiotoxicity in humans, a dose-dependent comparison was made between the predicted unbound blood concentration of ibogaine and noribogaine considering their TEF values. Figure 7 shows that, upon dosing ibogaine, the
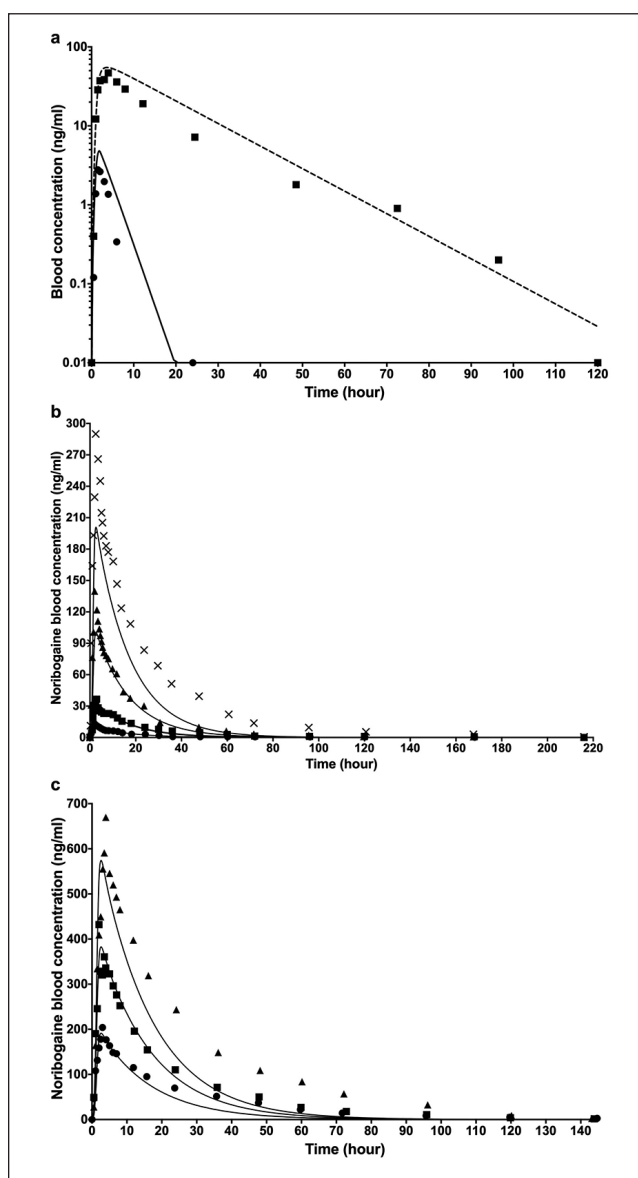

Fig. 6: Comparison of blood concentration-time curves of ibogaine and noribogaine in humans predicted with the PBK model and as published in the literature for human case studies

(a) Dots and squares respectively indicate the reported blood concentrations of ibogaine and noribogaine after a single oral dose of 20 mg ibogaine (Glue et al., 2015b). Solid lines and dashed lines represent the predictions for ibogaine and noribogaine, respectively. (b) Dots, squares, triangles and crosses represent the reported blood concentrations after an oral dose of 3, 10, 30 and 60 mg noribogaine (Glue et al., 2015a), respectively, with the solid lines being the predicted blood concentrations for the corresponding doses. (c) Dots, squares and triangles represent the reported blood concentrations after an oral dose of 60, 120 and 180 noribogaine (Glue et al., 2016), respectively, with the solid lines being the predicted blood concentrations of the corresponding doses.

Tab. 2: Summary of *in vivo* kinetic studies and evaluation of the PBK model predictions for ibogaine and noribogaine blood C_{max} and AUC

Compound	Mean body weight (kg)	Mean dose (mg/day)	*In vivo* C_{max} (ng/mL)[a]	Predicted C_{max} (ng/mL)	Ratio predicted C_{max}/ *in vivo* C_{max}	*In vivo* AUC (ng*h/ mL)[a]	Predicted AUC (ng*h/mL)	Ratio predicted AUC/ *in vivo* AUC	Reference
Ibogaine	80[b]	20	2.75	4.80	1.7	9.0	19.2	2.1	Glue et al., 2015b
Noribogaine		-[c]	46.8	54.8	1.2	693.5	1027.1	1.5	
Noribogaine	78	3	13.0	10.0	0.77	185.5	165.8	0.89	Glue et al., 2015b
		10	36.3	33.5	0.92	636.25	552.8	0.87	
		30	139.8	100.4	0.72	1751.0	1658.4	0.95	
		60	290.0	200.8	0.69	4905.5	3316.9	0.68	
Noribogaine	81.9	60	204.0	191.3	0.94	5150.8	3924.1	0.76	Glue et al., 2015b
		120	432.0	382.7	0.89	8201.3	7848.5	0.96	
		180	669.8	574.1	0.86	17219.3	11773.3	0.68	

[a] Blood data were obtained by multiplying reported plasma data by the BPr value. [b] Body weight was not reported and set equal to the average of values in other studies conducted by the same group (Glue et al., 2016; Glue et al., 2015a), assuming subjects have similar demographic characteristics. [c] Subjects were administered ibogaine.

contribution of noribogaine to the C_{max} expressed in unbound ibogaine equivalents is substantially higher than the contribution of ibogaine itself at all dose levels evaluated. The relative contribution of ibogaine to the ibogaine equivalents increases with increasing oral dose but is still about 8-fold lower than that of noribogaine at 500 mg despite the only limited difference in the TEF value between the two compounds. This observation can be ascribed to the fact that the concentration of noribogaine is higher than that of ibogaine (see also Fig. 6a) due to the fact that the catalytic efficiency of ibogaine O-demethylation to noribogaine is more efficient than the clearance of noribogaine by glucuronidation.

3.6 QIVIVE using PBK modeling-based reverse dosimetry, its validation and BMD analysis

By applying reverse dosimetry, the *in vitro* concentration-response curves of ibogaine and noribogaine obtained in the hiPSC-CM MEA assay were translated to predicted *in vivo* dose-response curves for the QTc prolongation upon oral administration of ibogaine (Fig. 8a) or noribogaine (Fig. 8b). Subsequently, the predicted data were compared to the *in vivo* dose-response data for QTc prolongation obtained from case studies and clinical studies to evaluate the performance of the PBK modeling-based reverse dosimetry predictions (Fig. 8). Given the unknown purity of internet-purchased ibogaine described in the case studies, a range of 15 to 50% was used to correct for the effective doses. Figure 8a reveals that the predicted dose-dependent QTc prolongation for ibogaine is best in line with the reported data when a purity of 15% is considered. For noribogaine, the predicted dose-response curve is comparable with the reported dose-response data on QTc prolongation (Fig. 8b).
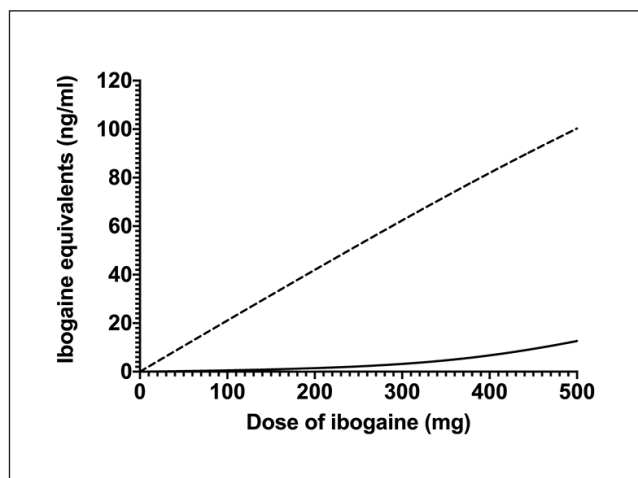
Fig. 7: Predicted dose-dependent relative contribution of ibogaine (solid line) and noribogaine (dashed line) to the C_{max} expressed in unbound ibogaine equivalents for 70 kg body weight

To further evaluate the model predictions and derive PoDs for risk assessment, $BMDL_{10}$ values were calculated from both predicted and reported dose-response curves. The $BMDL_{10}$ value of noribogaine derived from the clinical study of Glue et al. (2016) was 163 mg for the subjects with an average body weight of 81.9 kg, which is 1.5-fold higher than the predicted $BMDL_{10}$ value, amounting to 110 mg for an 81.9 kg person. This shows that PBK modeling-based reverse dosimetry can adequately predict the *in vivo* cardiotoxicity of noribogaine. The predicted $BMDL_{10}$ value
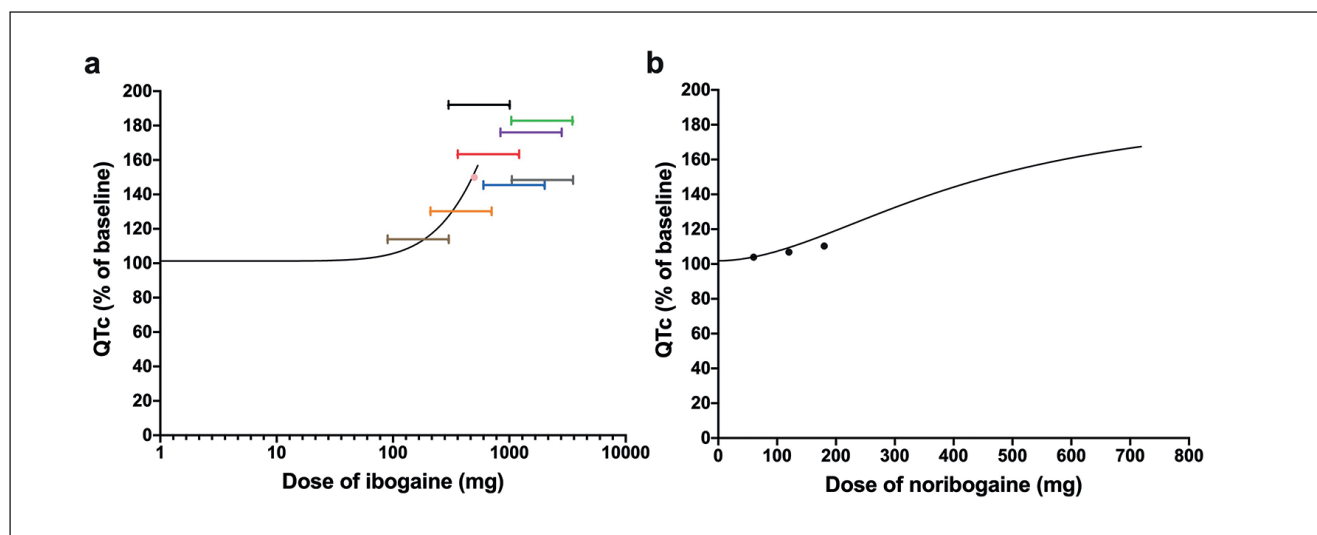
Fig. 8: Predicted dose-response curves for cardiotoxicity of (a) ibogaine and (b) noribogaine obtained using PBK modeling-based reverse dosimetry compared to *in vivo* human data derived from literature

The curves represent the predicted dose-dependent QTc prolongation. Horizontal bars or the dot in (a) represent the reported data of ibogaine obtained from the following studies: Asua (2013) (grey); Grogan et al. (2019) (black); Henstra et al. (2017) (orange); Hildyard et al. (2016) (green); Hoelen et al. (2009) (pink dot); Meisner et al. (2016) (blue); Pleskovic et al. (2012) (brown); Steinberg and Deyell (2018) (purple); Vlaanderen et al. (2014) (red). The horizontal bars represent the range of effective doses corrected by multiplying the reported doses with the purity range of internet-purchased ibogaine (15-50%) (Alper et al., 2012). Dots in (b) represent the *in vivo* dose-response data for noribogaine reported in Glue et al. (2016).

for ibogaine-induced QTc prolongation was 108 mg for 70 kg body weight, which is similar to that for noribogaine (94.2 mg, based on 70 kg body weight), indicating a comparable potency of the two compounds in inducing QTc prolongation.

4 Discussion and conclusion

The aim of the present study was to provide additional proof-of-principle for the prediction of potential human cardiotoxicity via QTc prolongation by combining an *in vitro* cardiotoxicity assay, *in vitro*-derived biokinetic parameters, and PBK modeling-based reverse dosimetry into a NAM for human risk and safety assessment. Two herbal alkaloids, ibogaine and noribogaine, which are promising anti-addiction drugs, were selected as model compounds since their cardiotoxicity is a major safety concern related to their clinical use, while so far not well studied. In addition, available *in vivo* kinetic and QTc data available for human subjects who had been exposed to the compounds enabled the evaluation of the developed NAM against clinically observed responses.

In the current paper, the electrophysiological cardiotoxicity of ibogaine and noribogaine was assessed using hiPSC-CMs on a MEA platform, which has been used previously for detecting drug-induced QTc prolongation and proarrhythmia (Shi et al., 2020a,b; Satsuka and Kanda, 2020). The results reveal that ibogaine and noribogaine prolong the FPDc in a concentration-dependent manner, which could be explained by their inhibitory

effects on hERG channels as detected using human mammalian cell lines heterologously expressing hERG channels (Alper et al., 2016; Koenig et al., 2014; Rubi et al., 2017). We also found that ibogaine was 1.4-fold more potent than noribogaine in prolonging FPDc, which is in contrast to the hERG inhibition studies, which reported a lower (1.3-fold) potency of ibogaine compared to noribogaine. The discrepancy might be ascribed to the use of different cell models. Unlike the transfected cell lines overexpressing a single type of ion channel, hiPSC-CMs express the major cardiac ion channels and receptors present in human cardiomyocytes (Karakikes et al., 2015; Kussauer et al., 2019; Ma et al., 2011), and thus the observed results of ibogaine and noribogaine could be the result of multiple ion-channel effects. Rubi et al. (2017) assessed the cardiotoxicity of ibogaine and noribogaine in hiPSC-CMs using one concentration of each compound that prolonged the action potential duration at 90% repolarization by respectively 14.2% and 15.5%, indicating comparable potency. Additionally, arrhythmia-type waveforms were observed upon treatment of hiPSC-CMs with ibogaine at high concentrations, which is in line with case studies where cardiac arrhythmia has been associated with the intake of an overdose of ibogaine (Asua, 2013; Paling et al., 2012).

Furthermore, at clinically relevant doses of ibogaine for the treatment of drug addiction (typically 500-1000 mg), the total blood concentration of noribogaine ranged from 0.7 to 4.5 µM (Mash et al., 2018), and unbound blood concentrations ranged from 0.08 to 0.47 µM when taking the unbound fraction in plasma and BPr into account. These values cover the unbound *in vi-*

tro effective concentration (BMCL$_{10}$) of noribogaine of 0.12 µM, a value corrected for the unbound fraction in the *in vitro* medium obtained in the current study, indicating that the cardiotoxicity of noribogaine contributes to ibogaine-induced cardiotoxicity and should thus be considered in the reverse dosimetry.

Results obtained from *in vitro* microsomal incubations reveal a high catalytic efficiency for the metabolism of ibogaine to noribogaine, which is in accordance with published data indicating that ibogaine is a compound with high intrinsic clearance with the majority being metabolized to noribogaine (Obach et al., 1998). Based on studies with human liver microsomes, Obach et al. (1998) suggested that two enzymes with different activities were involved in the formation of noribogaine, and the apparent V$_{max}$ and K$_m$ for the high-affinity enzyme appeared comparable with our data. However, the reported biphasic kinetics were not observed in our incubations. Furthermore, we found that the catalytic efficiency for the conversion of noribogaine to noribogaine glucuronide was quite low, which is consistent with the fact that only small amounts of noribogaine glucuronides were reported to be formed following an oral dose of noribogaine (Glue et al., 2015a). The substantially higher catalytic efficiency for conversion of ibogaine to noribogaine than for glucuronidation of noribogaine is also reflected in the kinetic data of the present study and explains why upon dosing ibogaine, plasma levels of noribogaine exceed those of ibogaine itself. Additionally, by comparing the unbound blood concentration corrected for TEF values of ibogaine and noribogaine, we found that noribogaine is predicted to be a major contributor to the unbound TEQ concentration expressed in ibogaine equivalents. Therefore, it can be speculated that noribogaine instead of ibogaine itself plays a dominant role in the *in vivo* cardiotoxicity upon the oral administration of ibogaine. The discrepancy between the relatively high cardiotoxic potency of ibogaine observed in the hiPSC-CM MEA assay and a relatively small contribution to the *in vivo* cardiotoxicity could be explained by our findings that i) ibogaine can be efficiently and extensively metabolized to noribogaine, ii) ibogaine highly binds to the plasma protein, resulting in a low unbound internal concentration of ibogaine, which is the fraction generally assumed to be responsible for the therapeutic or toxic effect of drugs (Smith et al., 2010), iii) clearance of noribogaine to its glucuronide is less efficient, and iv) the protein binding of noribogaine is somewhat less than that of ibogaine, resulting in higher unbound concentrations.

The blood C$_{max}$ and AUC values of ibogaine and noribogaine predicted by the PBK model are comparable with the literature data, with differences between the predicted and reported values being less than 2-fold, indicating an adequate predictive performance of the developed PBK models.

Based on the sensitivity analysis (Text S3[1]), the influence of metabolic parameters on the predicted C$_{max}$ of ibogaine in heart venous blood showed a dose-dependent change. When the oral dose of ibogaine increased to 500 mg, the influence of V$_{max}$ increased while K$_m$ was less influential. This may be explained by the fact that at high dose levels metabolism gets saturated, which reduces the influence of the K$_m$ with metabolic clearance being dependent on V$_{max}$. It is also of interest to note that most of the

ibogaine related parameters, including metabolic parameters, were not influential to the unbound TEQ concentration expressed in ibogaine equivalents, which however was sensitive to noribogaine related parameters. Furthermore, results show that the unbound TEQ concentration and C$_{max}$ of noribogaine in the heart venous blood were affected by these noribogaine related parameters to a similar extent.

Upon evaluation of the newly defined PBK models, they were used to translate the *in vitro* concentration response curves obtained in the hiPSC-CM-MEA assay to *in vivo* dose response curves for cardiotoxicity of ibogaine and noribogaine. To evaluate the predictions of the PBK modeling-based reverse dosimetry NAM, the predicted dose-response curves of ibogaine and noribogaine were compared to available *in vivo* data. The results obtained show that the predicted dose-response curve for ibogaine is in line with the reported QTc prolongation data, especially when the reported doses were corrected for a purity of 15%, which could be considered as a representative and realistic purity of internet-purchased ibogaine as reported by Hoelen et al. (2009). It is important to note the large variation in QTc prolongation data at similar oral doses observed in some case reports, which may be related to the individuals' diverse demographic characteristics and/or potential QTc prolonging risk factors, which were not well-documented in these studies. When applicable, applying exclusion or inclusion criteria to the reported data may better illustrate the dose-dependent effects of ibogaine and thus further improve the accuracy of the evaluation. For noribogaine, the predicted dose-response curve matches well with reported dose-response curves for QTc prolongation, with a difference in the BMDL$_{10}$ values derived from the predicted and reported data being less than 1.5-fold, which further demonstrates that the developed QIVIVE approach can adequately predict the *in vivo* cardiotoxicity for humans.

Based on human experiences, the administered dose of ibogaine for treating drug addiction has a wide range and varies from 6 to 30 mg/kg body weight (equal to 420 to 2100 mg for 70 kg body weight) (Alper et al., 1999; Davis et al., 2017; Mash et al., 2018; Noller et al., 2018; Schep et al., 2016). These dose levels are 4-to 21-fold higher than our predicted BMDL$_{10}$ value (96.9 mg for 70 kg body weight) for the ibogaine dependent induction of QTc prolongation. Since a BMDL$_{10}$ value generally represents a dose level at which the adverse effect is considered negligible (EFSA, 2017), the prolonged QTc would be expected at doses higher than the predicted BMDL$_{10}$ values, which is in line with the observation that QTc prolongations and arrythmia were observed in the subjects administered dose levels of ibogaine above the predicted BMDL$_{10}$ and that doses higher than 20 mg/kg bw ibogaine (equal to 1400 mg for 70 kg body weight) were associated with fatalities (Mash et al., 2018). Our predictions also confirm that ECG monitoring is essential for patients receiving ibogaine (Glue et al., 2016). In addition, many studies demonstrate that ibogaine and noribogaine have different neurobiological profiles (Baumann et al., 2001a,b; Maciulaitis et al., 2008), indicating that noribogaine might be more efficient than ibogaine in mediating certain pharmacological effects (Mash et al., 2016). Based on our model predictions and reported obser-

vations (Glue et al., 2016), a 1.2 to 1.6-fold higher dose of ibogaine is needed to reach the same C_{max} of noribogaine compared to the direct intake of noribogaine. Considering a similar *in vivo* potency observed in the current study for the predicted *in vivo* induction of the unwanted side effect of QTc prolongation by the two compounds (similar predicted $BMDL_{10}$ values), noribogaine would be a safer option.

In the present study, we consider that the relatively small contribution of ibogaine itself to the *in vivo* cardiotoxicity could be due to its low unbound fraction in plasma and its extensive metabolism. However, as ibogaine is a basic compound, the plasma protein binding could be influenced by the level of α1-acid glycoprotein, which has an up to 10-fold variation in human plasma (Smith and Waters, 2019). Furthermore, it has been reported that the internal concentration of ibogaine was up to 43-fold higher in poor CYP2D6 metabolizers compared to extensive metabolizers (Mash et al., 2001; Glue et al., 2015b). Glue et al. (2015b) also reported that the C_{max} of ibogaine was 26-fold higher in CYP2D6 extensive metabolizers who took CYP2D6 inhibitors compared to the ones who took placebo. Based on these observations, the cardiotoxicity of ibogaine might be more apparent in these sensitive individuals. Moreover, due to limited information on the metabolism of noribogaine, only the glucuronidation was included in the current model. Other metabolic reactions such as sulfation might also be involved in the clearance of noribogaine (Glue et al., 2016). Considering the relatively high potency of noribogaine in *in vivo* cardiotoxicity, it would be of interest to have a comprehensive metabolic profile for noribogaine defining also potential minor pathways for its clearance.

Based on findings in the present study, the developed *in vitro*-PBK modeling based approach could be extended to a higher throughput NAM for a broader range of chemicals inducing QTc prolongation, which ultimately would contribute to the use of non-animal based NAMs for human cardiac risk assessment and safety evaluations of chemicals. This can be achieved by employing a higher-throughput platform of the MEA (e.g., 96-well plate) (Kraushaar and Guenther, 2019), which allows the hiPSC-CM MEA assay to be used for rapidly detecting cardiotoxicity for large numbers of chemicals. Additionally, the development of a generic PBK model that only includes a limited number of, and thus the most influential, input parameters could accelerate the efficiency of PBK modeling, contributing to enhancing the throughput of the developed NAM. As illustrated in the present study and based on the sensitivity analysis (Text S3[1]), such input information could include physicochemical parameters, intestinal permeability, unbound fraction in plasma, and kinetic parameters for hepatic metabolic clearance. The development of high-throughput biokinetic assays to derive these parameters would further contribute to the efficiency of model parameterization

In conclusion, we have demonstrated that integrating *in vitro* cardiotoxicity data obtained with hiPSC-CMs in the MEA assay, *in vitro* biokinetic data, and PBK modeling can be a promising NAM to predict the *in vivo* dose-dependent cardiotoxicity of ibogaine and noribogaine in humans. Comparison of the predictions with the available *in vivo* data indicated the adequate performance of the developed *in vitro-in silico* approach. Obtained predictions also reveal a similar *in vivo* cardiotoxicity potency upon oral administration of ibogaine and noribogaine, while noribogaine might play a substantial role in ibogaine-induced QTc prolongation. Altogether, the present study shows additional proof-of-principle for using a NAM consisting of PBK modeling-based reverse dosimetry of hiPSC-CM MEA assay data for the prediction of human cardiotoxicity, which can be used for cardiac safety evaluation.

References

Abdullah, R., Alhusainy, W., Woutersen, J. et al. (2016). Predicting points of departure for risk assessment based on in vitro cytotoxicity data and physiologically based kinetic (PBK) modeling: The case of kidney toxicity induced by aristolochic acid I. *Food Chem Toxicol 92*, 104-116. doi:10.1016/j.fct.2016.03.017

Alper, K. R., Lotsof, H. S., Geerte, M. N. et al. (1999). Treatment of acute opioid withdrawal with ibogaine. *Am J Addict 8*, 234-242. doi:10.1080/105504999305848

Alper, K. R., Stajić, M. and Gill, J. R. (2012). Fatalities temporally associated with the ingestion of ibogaine. *J Forensic Sci 57*, 398-412. doi:10.1111/j.1556-4029.2011.02008.x

Alper, K. R., Bai, R., Liu, N. et al. (2016). hERG blockade by iboga alkaloids. *Cardiovasc Toxicol 16*, 14-22. doi:10.1007/s12012-015-9311-5

Andersen, M. E., McMullen, P. D., Phillips, M. B. et al. (2019). Developing context appropriate toxicity testing approaches using new alternative methods (NAMs). *ALTEX 36*, 523-534. doi:10.14573/altex.1906261

Ando, H., Yoshinaga, T., Yamamoto, W. et al. (2017). A new paradigm for drug-induced torsadogenic risk assessment using human iPS cell-derived cardiomyocytes. *J Pharmacol Toxicol Methods 84*, 111-127. doi:10.1016/j.vascn.2016.12.003

Asua, I. (2013). Growing menace of ibogaine toxicity. *British J Anaesth 111*, 1029-1030. doi:10.1093/bja/aet396

Badhan, R. K., Gittins, R. and Al Zabit, D. (2019). The optimization of methadone dosing whilst treating with rifampicin: A pharmacokinetic modeling study. *Drug Alcohol Depend 200*, 168-180. doi:10.1016/j.drugalcdep.2019.03.013

Baumann, M. H., Pablo, J., Ali, S. F. et al. (2001a). Comparative neuropharmacology of ibogaine and its O-desmethyl metabolite, noribogaine. *Alkaloids Chem Biol 56*, 79-113. doi:10.1016/S0099-9598(01)56009-5

Baumann, M. H., Rothman, R. B., Pablo, J. P. et al. (2001b). In vivo neurobiological effects of ibogaine and its O-desmethyl metabolite, 12-hydroxyibogamine (noribogaine), in rats. *J Pharmacol Exp Ther 297*, 531-539.

Bentz, J., O'Connor, M. P., Bednarczyk, D. et al. (2013). Variability in P-glycoprotein inhibitory potency (IC_{50}) using various in vitro experimental systems: Implications for universal digoxin drug-drug interaction risk assessment decision criteria. *Drug Metab Dispos 41*, 1347-1366. doi:10.1124/dmd.112.050500

Bos, P. M., Geraets, L., de Wit-Bos, L. et al. (2020). Towards

an animal-free human health assessment: Starting from the current regulatory needs. *ALTEX 37*, 395-408. doi:10.14573/altex.1912041

Brown, R. P., Delp, M. D., Lindstedt, S. L. et al. (1997). Physiological parameter values for physiologically based pharmacokinetic models. *Toxicol Ind Health 13*, 407-484. doi:10.1177/074823379701300401

Chang, Y., Fang, W. B., Lin, S. N. et al. (2011). Stereo-selective metabolism of methadone by human liver microsomes and cDNA-expressed cytochrome P450s: A reconciliation. *Basic Clin Pharmacol Toxicol 108*, 55-62. doi:10.1111/j.1742-7843.2010.00628.x

Davis, A. K., Barsuglia, J. P., Windham-Herman, A. M. et al. (2017). Subjective effectiveness of ibogaine treatment for problematic opioid consumption: Short-and long-term outcomes and current psychological functioning. *J Psychedelic Stud 1*, 65-73. doi:10.1556/2054.01.2017.009

EFSA – European Food Safety Authority (2017). Update: Use of the Benchmark Dose Approach in Risk Assessment. doi:10.2903/j.efsa.2017.4658

Fisher, M. B., Campanale, K., Ackermann, B. L. et al. (2000). In vitro glucuronidation using human liver microsomes and the pore-forming peptide alamethicin. *Drug Metab Dispos 28*, 560-566.

Florian, J., Garnett, C., Nallani, S. et al. (2012). A modeling and simulation approach to characterize methadone QT prolongation using pooled data from five clinical trials in MMT patients. *Clin Pharmacol Ther 91*, 666-672. doi:10.1038/clpt.2011.273

Foster, D. J., Somogyi, A. A., Dyer, K. R. et al. (2000). Steady-state pharmacokinetics of (R)- and (S)-methadone in methadone maintenance patients. *Br J Clin Pharmacol 50*, 427-440. doi:10.1046/j.1365-2125.2000.00272.x

Ferruzza, S., Rossi, C., Sambuy, Y. et al. (2013). Serum-reduced and serum-free media for differentiation of Caco-2 cells. *ALTEX 30*, 159-168. doi:10.14573/altex.2013.2.159

Gilbert-Sandoval, I., Wesseling, S. and Rietjens, I. M. C. M. (2020). Predicting the acute liver toxicity of aflatoxin B1 in rats and humans by an in vitro-in silico testing strategy. *Mol Nutr Food Res 64*, e2000063. doi:10.1002/mnfr.202000063

Glue, P., Lockhart, M., Lam, F. et al. (2015a). Ascending-dose study of noribogaine in healthy volunteers: Pharmacokinetics, pharmacodynamics, safety, and tolerability. *J Clin Pharmacol 55*, 189-194. doi:10.1002/jcph.404

Glue, P., Winter, H., Garbe, K. et al. (2015b). Influence of CYP2D6 activity on the pharmacokinetics and pharmacodynamics of a single 20 mg dose of ibogaine in healthy volunteers. *J Clin Pharmacol 55*, 680-687. doi:10.1002/jcph.471

Glue, P., Cape, G., Tunnicliff, D. et al. (2016). Ascending single-dose, double-blind, placebo-controlled safety study of noribogaine in opioid-dependent patients. *Clin Pharmacol Drug Dev 5*, 460-468. doi:10.1002/cpdd.254

Goutarel, R., Gollnhofer, O. and Sillans, R. (1993). Pharmacodynamics and therapeutic applications of iboga and ibogaine. *Psychedelic Monogr Essays 6*, 71-111. https://ibogainedossier.com/bwiti1.html

Grogan, J., Gerona, R., Snow, J. W. et al. (2019). Ibogaine consumption with seizure-like episodes, QTc-prolongation, and captured cardiac dysrhythmias. *J Emerg Med 57*, e99-e104. doi:10.1016/j.jemermed.2019.06.05

Henstra, M., Wong, L., Chahbouni, A. et al. (2017). Toxicokinetics of ibogaine and noribogaine in a patient with prolonged multiple cardiac arrhythmias after ingestion of internet purchased ibogaine. *Clin Toxicol 55*, 600-602. doi:10.1080/15563650.2017.1287372

Hildyard, C., Macklin, P., Prendergast, B. et al. (2016). A case of QT prolongation and torsades de pointes caused by ibogaine toxicity. *J Emerg Med 50*, e83-e87. doi:10.1016/j.jemermed.2015.06.05

Hoelen, D. W., Spiering, W. and Valk, G. D. (2009). Long-QT syndrome induced by the antiaddiction drug ibogaine. *N Engl J Med 360*, 308-309. doi:10.1056/NEJMc0804248

Hubatsch, I., Ragnarsson, E. G. and Artursson, P. (2007). Determination of drug permeability and prediction of drug absorption in Caco-2 monolayers. *Nat Protoc 2*, 2111. doi:10.1038/nprot.2007.303

ICCVAM – Interagency Coordinating Committee on the Validation of Alternative Methods (2018). A Strategic Roadmap for Establishing New Approaches to Evaluate the Safety of Chemicals and Medical Products in the United States. doi:10.22427/NTP-ICCVAM-ROADMAP2018

ICH – The International Council for Harmonisation of Technical Requirements for Pharmaceuticals for Human Use (2005). E14: The Clinical Evaluation of QT/QTc Interval Prolongation and Proarrhythmic Potential for Non-Antiarrhythmic Drugs. https://database.ich.org/sites/default/files/E14_Guideline.pdf (accessed 20.01.2021)

Karakikes, I., Ameen, M., Termglinchan, V. et al. (2015). Human induced pluripotent stem cell-derived cardiomyocytes: Insights into molecular, cellular, and functional phenotypes. *Circ Res 117*, 80-88. doi:10.1161/CIRCRESAHA.117.305365

Kitaguchi, T., Moriyama, Y., Taniguchi, T. et al. (2017). CSAHi study: Detection of drug-induced ion channel/receptor responses, QT prolongation, and arrhythmia using multi-electrode arrays in combination with human induced pluripotent stem cell-derived cardiomyocytes. *J Pharmacol Toxicol Methods 85*, 73-81. doi:10.1016/j.vascn.2017.02.001

Koenig, X., Kovar, M., Boehm, S. et al. (2014). Anti-addiction drug ibogaine inhibits hERG channels: A cardiac arrhythmia risk. *Addict Biol 19*, 237-239. doi:10.1111/j.1369-1600.2012.00447.x

Kraushaar, U. and Guenther, E. (2019). Assay procedures for compound testing of hiPSC-derived cardiomyocytes using multiwell microelectrode arrays cell-based assays using iPSCs for drug development and testing. In C. F. Mandenius and J. Ross (eds.), *Cell-Based Assays Using iPSCs for Drug Development and Testing* (197-208). Methods in Molecular Biology 1994. New York, NY, USA: Humana. doi:10.1007/978-1-4939-9477-9_18

Kussauer, S., David, R. and Lemcke, H. (2019). hiPSCs derived cardiac cells for drug and toxicity screening and disease mod-

eling: What micro-electrode-array analyses can tell us. *Cells 8*, 1331. doi:10.3390/cells8111331

Litjens, R. P. and Brunt, T. M. (2016). How toxic is ibogaine? *Clin Toxicol 54*, 297-302. doi:10.3109/15563650.2016.1138226

Louisse, J., de Jong, E., van de Sandt, J. J. et al. (2010). The use of in vitro toxicity data and physiologically based kinetic modeling to predict dose-response curves for in vivo developmental toxicity of glycol ethers in rat and man. *Toxicol Sci 118*, 470-484. doi:10.1093/toxsci/kfq270

Ma, J., Guo, L., Fiene, S. J. et al. (2011). High purity human-induced pluripotent stem cell-derived cardiomyocytes: Electrophysiological properties of action potentials and ionic currents. *Am J Physiol Heart Circ Physiol 301*, H2006-H2017. doi:10.1152/ajpheart.00694.2011

Maciulaitis, R., Kontrimaviciute, V., Bressolle, F. et al. (2008). Ibogaine, an anti-addictive drug: Pharmacology and time to go further in development. A narrative review. *Hum Exp Toxicol 27*, 181-194. doi:10.1177/0960327107087802

Martin, R. L., McDermott, J. S., Salmen, H. J. et al. (2004). The utility of hERG and repolarization assays in evaluating delayed cardiac repolarization: Influence of multi-channel block. *J Cardiovasc Pharmacol 43*, 369-379. doi:10.1097/00005344-200403000-00007

Mash, D. C., Kovera, C. A., Pablo, J. et al. (2001). Ibogaine in the treatment of heroin withdrawal. *Alkaloids Chem Biol 56*, 155-171. doi:10.1016/S0099-9598(01)56012-5

Mash, D. C., Ameer, B., Prou, D. et al. (2016). Oral noribogaine shows high brain uptake and anti-withdrawal effects not associated with place preference in rodents. *J Psychopharmacol 30*, 688-697. doi:10.1177/0269881116641331

Mash, D. C., Duque, L., Page, B. et al. (2018). Ibogaine detoxification transitions opioid and cocaine abusers between dependence and abstinence: Clinical observations and treatment outcomes. *Front Pharmacol 9*, 529. doi:10.3389/fphar.2018.00529

Meisner, J. A., Wilcox, S. R. and Richards, J. B. (2016). Ibogaine-associated cardiac arrest and death: Case report and review of the literature. *Ther Adv Psychopharmacol 6*, 95-98. doi:10.1177/2045125315626073

Mujtaba, S., Romero, J. and Taub, C. C. (2013). Methadone, QTc prolongation and torsades de pointes: Current concepts, management and a hidden twist in the tale? *J Cardiovasc Dis Res 4*, 229-235. doi:10.1016/j.jcdr.2013.10.001

Ning, J., Louisse, J., Spenkelink, B. et al. (2017). Study on inter-ethnic human differences in bioactivation and detoxification of estragole using physiologically based kinetic modeling. *Arch Toxicol 91*, 3093-3108. doi:10.1007/s00204-017-1941-x

Noller, G. E., Frampton, C. M. and Yazar-Klosinski, B. (2018). Ibogaine treatment outcomes for opioid dependence from a twelve-month follow-up observational study. *Am J Drug Alcohol Abuse 44*, 37-46. doi:10.1080/00952990.2017.1310218

Nozaki, Y., Honda, Y., Watanabe, H. et al. (2017). CSAHi study-2: Validation of multi-electrode array systems (MEA60/2100) for prediction of drug-induced proarrhythmia using human iPS cell-derived cardiomyocytes: Assessment of reference compounds and comparison with non-clinical studies and clinical information. *Regul Toxicol Pharmacol 88*, 238-251. doi:10.1016/j.yrtph.2017.06.006

O'Connell, C. W., Gerona, R. R, Friesen, M. W. et al. (2015). Internet-purchased ibogaine toxicity confirmed with serum, urine, and product content levels. *Am J Emerg Med 33*, 985.e5-e6. doi:10.1016/j.ajem.2014.12.023

Obach, R. S, Pablo, J. and Mash, D. C. (1998). Cytochrome P4502D6 catalyzes the O-demethylation of the psychoactive alkaloid ibogaine to 12-hydroxyibogamine. *Drug Metab Dispos 26*, 764-768.

Ovics, P., Regev, D., Baskin, P. et al. (2020). Drug development and the use of induced pluripotent stem cell-derived cardiomyocytes for disease modeling and drug toxicity screening. *Int J Mol Sci 21*, 7320. doi:10.3390/ijms21197320

Paling, F., Andrews, L., Valk, G. et al. (2012). Life-threatening complications of ibogaine: Three case reports. *Neth J Med 70*, 422-424.

Pang, L., Sager, P., Yang, X. et al. (2019). Workshop report: FDA workshop on improving cardiotoxicity assessment with human-relevant platforms. *Circ Res 125*, 855-867. doi:10.1161/CIRCRESAHA.119.315378

Patterson, E. A., Whelan, M. P. and Worth, A. P. (2020). The role of validation in establishing the scientific credibility of predictive toxicology approaches intended for regulatory application. *Comput Toxicol 17*, 100144. doi:10.1016/j.comtox.2020.100144

Pleskovic, A., Gorjup, V., Brvar, M. et al. (2012). Ibogaine-associated ventricular tachyarrhythmias. *Clin Toxicol 50*, 157-157. doi:10.3109/15563650.2011.647031

Punt, A., Bouwmeester, H., Blaauboer, B. J. et al. (2020). New approach methodologies (NAMs) for human-relevant biokinetics predictions: Meeting the paradigm shift in toxicology towards an animal-free chemical risk assessment. *ALTEX 37*, 607-622. doi:10.14573/altex.2003242

Rietjens, I. M. C. M., Louisse, J. and Punt, A. (2011). Tutorial on physiologically based kinetic modeling in molecular nutrition and food research. *Mol Nutr Food Res 55*, 941-956. doi:10.1002/mnfr.201000655

Rohatgi, A. (2020). WebPlotDigitizer (Version 4.4) (Computer software). https://apps.automeris.io/wpd/

Rubi, L., Eckert, D., Boehm, S. et al. (2017). Anti-addiction drug ibogaine prolongs the action potential in human induced pluripotent stem cell-derived cardiomyocytes. *Cardiovasc Toxicol 17*, 215-218. doi:10.1007/s12012-016-9366-y

Sala, L., Ward-van Oostwaard, D., Tertoolen, L. G. et al. (2017). Electrophysiological analysis of human pluripotent stem cell-derived cardiomyocytes (hPSC-CMs) using multi-electrode arrays (MEAs). *J Vis Exp*, e55587. doi:10.3791/55587

Satsuka, A. and Kanda, Y. (2020). Cardiotoxicity assessment of drugs using human iPS cell-derived cardiomyocytes: Toward proarrhythmic risk and cardio-oncology. *Curr Pharm Biotechnol 21*, 765-772. doi:10.2174/1389201020666190628143345

Schep, L. J., Slaughter, R., Galea, S. et al. (2016). Ibogaine for

treating drug dependence. What is a safe dose? *Drug Alcohol Depend 166*, 1-5. doi:10.1016/j.drugalcdep.2016.07.005

Shi, M., Bouwmeester, H., Rietjens, I. M. C. M. et al. (2020a). Integrating in vitro data and physiologically based kinetic modeling-facilitated reverse dosimetry to predict human cardiotoxicity of methadone. *Arch Toxicol 94*, 2809-2827. doi:10.1007/s00204-020-02766-7

Shi, M., Tien, N. T., de Haan, L. et al. (2020b). Evaluation of in vitro models of stem cell-derived cardiomyocytes to screen for potential cardiotoxicity of chemicals. *Toxicol In Vitro 67*, 104891. doi:10.1016/j.tiv.2020.104891

Smith, D. A., Di, L. and Kerns, E. H. (2010). The effect of plasma protein binding on in vivo efficacy: Misconceptions in drug discovery. *Nat Rev Drug Discov 9*, 929-939. doi:10.1038/nrd3287

Smith, S. A. and Waters, N. J. (2019). Pharmacokinetic and pharmacodynamic considerations for drugs binding to alpha-1-acid glycoprotein. *Pharm Res 36*, 1-19. doi:10.1007/s11095-018-2551-x

Steinberg, C. and Deyell, M. W. (2018). Cardiac arrest after ibogaine intoxication. *J Arrhythm 34*, 455-457. doi:10.1002/joa3.12061

Strikwold, M., Spenkelink, B., de Haan, L. et al. (2017). Integrating in vitro data and physiologically based kinetic (PBK) modelling to assess the in vivo potential developmental toxicity of a series of phenols. *Arch Toxicol 91*, 2119-2133. doi:10.1007/s00204-016-1881-x

Taboureau, O., El M'Selmi, W. and Audouze, K. (2020). Integrative systems toxicology to predict human biological systems affected by exposure to environmental chemicals. *Toxicol Appl Pharmacol 405*, 115210. doi:10.1016/j.taap.2020.115210

van Liempd, S., Morrison, D., Sysmans, L. et al. (2011). Development and validation of a higher-throughput equilibrium dialysis assay for plasma protein binding. *J Lab Autom 16*, 56-67. doi:10.1016/j.jala.2010.06.002

Vandenberk, B., Vandael, E., Robyns, T. et al. (2016). Which QT correction formulae to use for QT monitoring? *J Am Heart Assoc 5*, e003264. doi:10.1161/JAHA.116.003264

Vlaanderen, L., Martial, L., Franssen, E. et al. (2014). Cardiac arrest after ibogaine ingestion. *Clin Toxicol 52*, 642-643. doi:10.3109/15563650.2014.927477

Waters, N. J., Jones, R., Williams, G. et al. (2008). Validation of a rapid equilibrium dialysis approach for the measurement of plasma protein binding. *J Pharm Sci 97*, 4586-4595. doi:10.1002/jps.21317

Wedam, E. F., Bigelow, G. E., Johnson, R. E. et al. (2007). QT-interval effects of methadone, levomethadyl, and buprenorphine in a randomized trial. *Arch Intern Med 167*, 2469-2475. doi:10.1001/archinte.167.22.2469

WHO – World Health Organization (2010). Characterization and Application of Physiologically Based Pharmacokinetic Models in Risk Assessment. https://www.inchem.org/documents/harmproj/harmproj/harmproj9.pdf

Wolff, K., Rostami-Hodjegan, A., Hay, A. et al. (2000). Population-based pharmacokinetic approach for methadone monitoring of opiate addicts: Potential clinical utility. *Addiction 95*, 1771-1783. doi:10.1046/j.1360-0443.2000.951217717.x

Zhao, S., Kamelia, L., Boonpawa, R. et al. (2019). Physiologically based kinetic modeling-facilitated reverse dosimetry to predict in vivo red blood cell acetylcholinesterase inhibition following exposure to chlorpyrifos in the Caucasian and Chinese population. *Toxicol Sci 171*, 69-83. doi:10.1093/toxsci/kfz134

Zwartsen, A., de Korte, T., Nacken, P. et al. (2019). Cardiotoxicity screening of illicit drugs and new psychoactive substances (NPS) in human iPSC-derived cardiomyocytes using microelectrode array (MEA) recordings. *J Mol Cell Cardiol 136*, 102-112. doi:10.1016/j.yjmcc.2019.09.007

Conflict of interest
All authors declare that they have no conflict of interest.

Acknowledgement